

54. E. I. Bichenkov, S. D. Gilev, A. M. Ryabchun, et al., "Shock-wave method of generation of megagauss magnetic fields," *Zh. Prikl. Mekh. Tekh. Fiz.*, No. 3 (1987).
55. K. Nagayama and T. Mashimo, "Explosive-driven magnetic flux cumulation by the propagation of shock compressed conductive region in highly porous metal powders," *J. Appl. Phys.*, 61, No. 10 (1987).
56. A. D. Sakharov, R. Z. Lyudaev, E. I. Smirnov, et al., "Magnetic cumulation," *Dokl. Akad. Nauk SSSR*, 165, No. 1 (1965).
57. C. M. Fowler, R. S. Caird, and W. B. Carn, "Production of very high magnetic fields by explosion," *J. Appl. Phys.*, 31, No. 3 (1960).
58. A. I. Pavlovskii, N. P. Kolokol'chikov, M. I. Dolotenko, et al., "Cascade magnetic cumulation generator of superstrong magnetic fields," in: *Superstrong Magnetic Fields: Proc-3rd Int. Conf. on the Generation of Megagauss Magnetic Fields*, Nauka, Moscow (1984).
59. A. I. Pavlovskii, A. I. Bykov, M. I. Dolotenko, et al., "Limiting value of reproducible magnetic field in cascade generator MC-1," in: *Megagauss Technology and Pulsed Power Applications: Proc. 4th Int. Conf. on Megagauss Magnetic Field Generation*, New York (1987).

STRUCTURE AND DYNAMICS OF A PLASMA PISTON IN RAIL-GUN ACCELERATORS
FOR SOLID OBJECTS

A. G. Anisimov, Yu. L. Bashkatov, and G. A. Shvetsov

UDC 538.4+533.95

In recent years, beginning with [1], investigators have paid considerable attention to the study of possible acceleration of dielectric solids by a plasma piston in rail-gun accelerators. One expects that this development process will remove the thermal limits on the speed of metal particles and obtain speeds considerably exceeding the experimental level achieved [2]. Papers have appeared whose authors have considered the possibility of, and discussed plans for equipment to accelerate particles of mass on the order of a gram to speeds of 12 [3], 15 [4, 5], 20 [6, 7], 25 [4, 6, 8], 50 km/sec [9], etc. However, it should be noted that, in spite of almost a decade since the publication of [1] and considerable efforts, there has been no substantial progress in the technology of obtaining high speeds. The experimental results are very modest and are at the level of those of [1].

At present it is generally accepted that the main causes limiting the attainment of high speed of macroparticles in rail-gun accelerators with a plasma piston are associated with erosion of the channel walls under the action of the high-power heat flux from the moving plasma piston and the current flowing in the circuit. Analysis of the critical gas density for which the surface temperature of the electrodes reaches the melt temperature shows [10] that one cannot achieve efficient acceleration of the body and avoid erosion of the electrodes. The effect of erosion of the electrodes is different. The presence of added mass leads to the appearance of "limiting" values of the speed of the accelerated particle independently of the mechanism of erosion [10], to redistribution of current in the plasma piston, and to separation of the latter from the accelerated body [11]. Among the causes

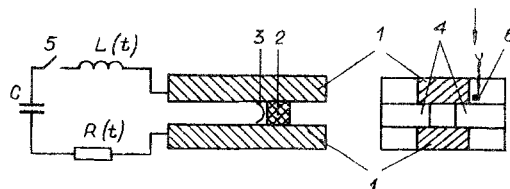


Fig. 1

Novosibirsk. Translated from *Zhurnal Prikladnoi Mekhaniki i Tekhnicheskoi Fiziki*, No. 2, pp. 145-150, March-April, 1989. Original article submitted August 4, 1988.



Fig. 2

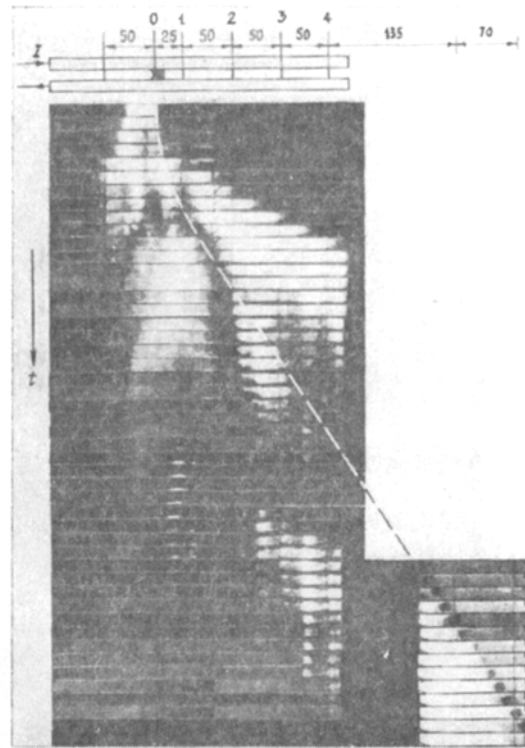


Fig. 3

leading to the plasma piston being separated from the accelerated body, [11] lists shunting of the current flowing directly through the accelerated body by metal evaporated from the electrodes (secondary discharges).

The full connection between erosion of the electrodes and the secondary discharges is not clear, but we think that from direct experiments one can conclude that there is a connection, especially if one postulates that in rail-gun accelerators of macroparticles with a plasma piston one meets conditions leading to the formation of high-speed, high-temperature jets of vapor from the material of the electrodes [12]. If this occurs in such a way that the generation and disappearance of the jets insert their special features into the structure of the plasma piston, in particular, this calls into question the possibility of accomplishing a magnetocompressive discharge in the accelerator, and this in turn leads to decrease of the force accelerating the body.

The aim of this work is to study the structure of the plasma piston. The experiments were conducted under conditions as close as possible to those in the experiments on acceleration of macroparticles [11, 13].

1. The scheme of the experiments is shown in Fig. 1, where C is a capacitor bank; $L(t)$ and $R(t)$ are the inductance and resistance of the circuit; 1, electrodes; 2, accelerated body; 3, a metal foil, 4, glass windows, and 5, a discharge switch. When the switch is operated the capacitor bank discharges in the rail-gun, the foil explodes, and a plasma piston is formed which moves under the action of the Lorentz force and accelerates the body.

In the experiments we used a capacitor bank of capacitance from 10.2 to 20.4 mF at a voltage of 5 kV. The amplitude and shape of the current pulse was assigned by choosing the initial voltage, the bank capacitance, and the initial circuit inductance. The amplitude of the currents was varied from 300 to 500 kA. To create the plasma we used a copper foil of thickness 30 μm . The length of the rail-gun was 250-400 mm, the electrode section was 19×10 mm, the height of the glass insulators was 10 mm, and the channel section was 10×9 mm. The accelerated body was made of Kapron. The size of the body was $10 \times 10 \times 9$ mm, and its mass was ~ 1 g.

In the experiments we recorded the current at the input to the rail-gun, and the voltage at its input and output. With the aid of inductance sensors we determined the current distribution in the plasma crosspiece. The main attention was paid to optical recording of the plasma piston. In a number of experiments we replaced the accelerated body with a dielectric suppressor. This allowed us to photograph the plasma piston under steady conditions.

2. The optical scheme shows that in the initial stage of a high-power discharge (roughly for 25-30 μsec) there were insignificant differences in the behavior of the plasma in the tests with the dielectric suppressor and the accelerated body. The plasma formed when the foil is exploded electrically undergoes complex changes under the action of the electromagnetic and gasdynamic forces. In both cases the length of the plasma plug increases immediately after the foil explodes. After a time of $\sim 10 \mu\text{sec}$ the plasma occupies a space of length $\sim 40 \text{ mm}$. Then the colder part is adjacent to the suppressor (or the body). The high-temperature part of the plasma stands off from the suppressor at a distance of 2-4 cm and for a time of 25-30 μsec remains roughly in one place, increasing only slightly in size, and executing a small number of spatial oscillations to and from the suppressor. Then the length of the plasma increases up to 5-7 cm, and in it appear individual hot sections (arcs and strata), whose lifetime varies in the range 1-10 μsec . Their number in the present experiments could not be counted and varies with time. Throughout the entire time of the optical record the magnetocompressive localized discharge regime is not achieved. In some experiments with the suppressor there is no erosion of the electrodes in the section 10-20 mm adjacent to the suppressor, but strong erosion is observed in a more distant section of the length up to 30 mm.

Figures 2-5 show photographs illustrating the development of the process with time in the experiments with an accelerated body, where 0 is the location of the foil and the accelerated body, and 1-5 are the inductance sensors. In the experiment (Fig. 2, time between frames 3.3 μsec) the channel is closed by a suppressor behind the body at a distance of 35 mm. From the photographs it can be seen that the plasma piston formed from the foil explo-

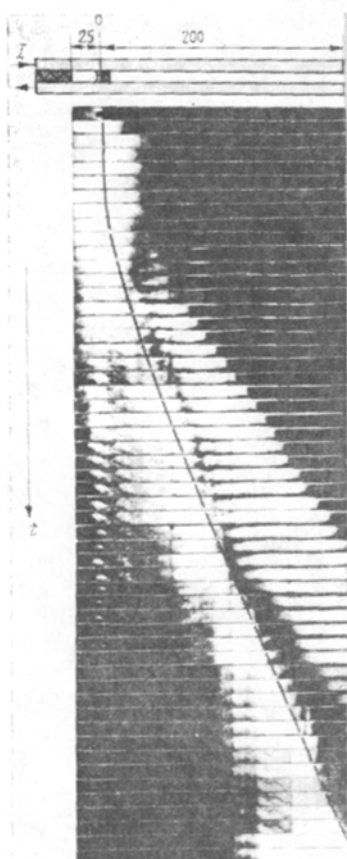


Fig. 4

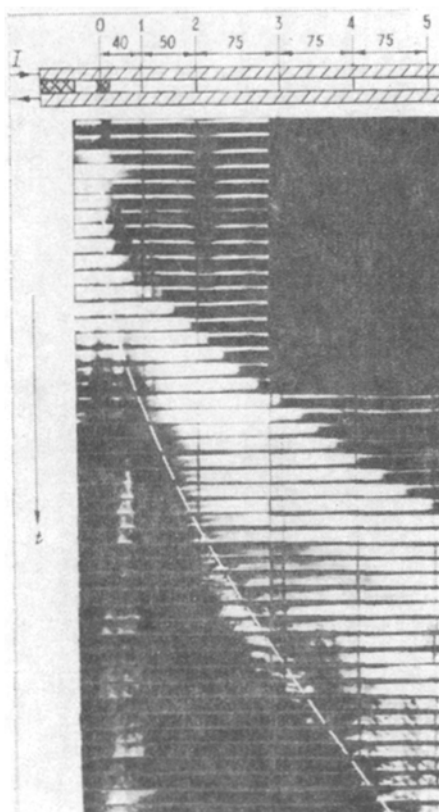


Fig. 5

sion increases in length rapidly in the direction opposite to the magnetic pressure forces. For the first 20-30 μsec the accelerated body practically does not change position.

In another experiment (Fig. 3, time between frames 8 μsec) the channel behind the body was open. In the photographs one can see a region of bright luminosity, of which the trailing boundary first propagates in the direction opposing the body motion, then stops, and later moves behind the accelerated body, continuously changing its form and internal picture of luminosity. The less-bright part of the plasma continues to expand in the direction opposite to the body motion, then breaks up into separate sections and stops glowing.

In the experiments conducted with a channel of square section with glass insulators we observed a breakthrough of the plasma ahead of the body roughly 30 μsec after explosion of the foil. The inductance sensors recorded current flow along the outburst of plasma.

The broken line in Fig. 4 (time between frames is 3.37 μsec) shows the trajectory of motion of the accelerated body. The speed of the forward boundary of the plasma as it exits from the rail-gun is ~ 2.2 km/sec, and the speed of the body is ~ 1.5 km/sec.

The broken line in Fig. 5 (time between frames is 4.5 μsec) shows the body trajectory, which intersects the zone where no luminosity is observed, but the inductance sensors show that the plasma piston is in this zone and that a large current is flowing along it. Evidently, in the region where there is no luminosity from the piston in the photographs the glass walls have lost their transparency. The dark bands are generated at the location of the foil and propagate to the adjacent sections. After a certain time (after breakdown of the glass walls) one sees the luminosity of the plasma that has been drawn out of the channel.

It can be seen from Fig. 3 that the part of the piston adjacent to the body gradually loses its luminosity, and from the initial location of the foil a new plasma plug is generated which accelerates the body even after it exits from the barrel of the rail-gun. It can be seen from the photographs that there is a reflected shock wave following the shock at the body from this plug.

In addition to the optical record of the plasma piston in the experiments we measured the current distribution in the piston. Magnetic probes were located near the rail-gun channel (Fig. 1; 6 is the magnetic probe). The direction of the sensor axis is shown by the arrow. Figure 6 shows oscillograms from the inductance sensors 1-5 in the experiment (see Fig. 5). The origin of the signals in all the oscillograms coincides with the arrival of the luminous plasma front which has trickled through ahead of the body. The arrows denote times of passage of the body past the sensors. It can be seen from the data presented that an estimate of the body speed from the readings of the inductance sensors and the luminosity of the plasma piston front may be incorrect.

Figure 7 shows the dependences of current vs. time at the rail-gun input (upper curve) and the integrated signals from the inductance sensors 1-5 in the experiment (see Fig. 5). From the graph one can estimate the current flowing at different times in the plasma that has broken through ahead of the body, that is coming behind the body, and passing in the arc at the foil location.

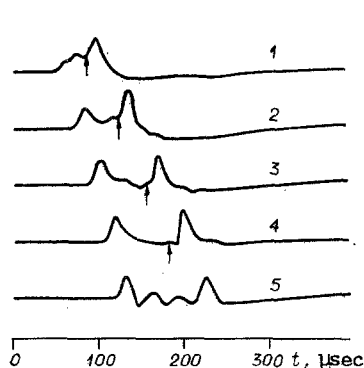


Fig. 6

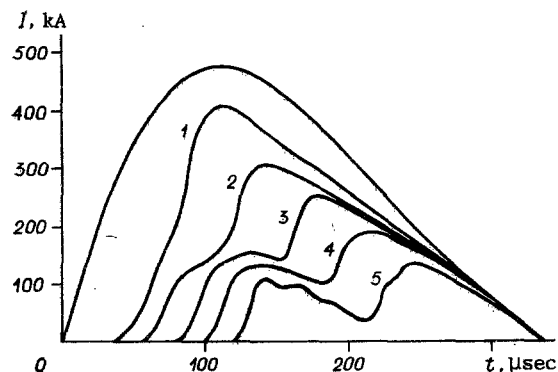


Fig. 7

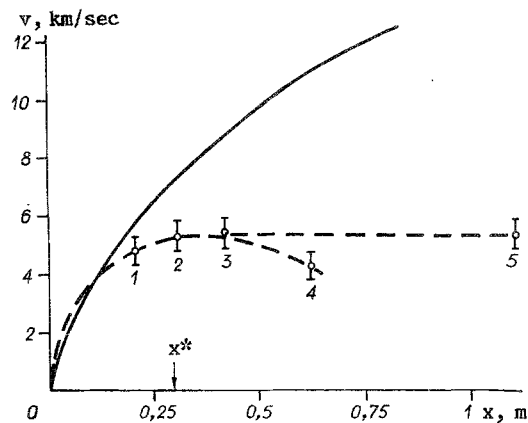


Fig. 8

In all the experiments (see Figs. 2-5) at the foil location the arc burns throughout the entire time of the optical record (≈ 200 μsec); in this location, and also at a distance of 30-35 mm upstream, we observe strong erosion of the electrodes. Later (upstream) the erosion is insignificant, but traces of strong thermal action on the electrodes are noticeable at distances up to 150 mm. In the direction of motion of the body on the electrodes one can see traces of the material of the electrodes.

Although the results presented in this study do not fully uncover the internal structure of the plasma piston, and are conditioned in the main by the specific conduct of the experiments, associated with the presence of glass insulators, they are general in nature, as shown by natural experiments on acceleration of macroparticles. Of course, in this case, with careful fabrication of the channel, and precision adjustment of the dimensions of the accelerated body to the dimensions of the channel one could avoid breakthrough of the plasma ahead of the body, but we were unable to accomplish a magnetocompressive discharge. The sensors show that as the body moves in the channel the length of the plasma plug continuously increases, there is a redistribution of the current along the plasma from the front to the rear, leading as an end result to separation (lagging) of the plasma from the accelerated body [11]. The plasma lag in the experiments with a circular rail-gun with a channel diameter of 5.7 mm in accelerating a body of mass 0.2 g is illustrated in Fig. 8 (1-4 are the speed of the plasma piston, determined from the signals of the inductance sensors, 5 is the optical record of the body speed, and 6 is the computed body speed from the current graph). An analogous picture occurs in accelerating macroparticles in a rail-gun of circular section of diameter 11.7 mm [11]. From the data obtained in this study one can conclude that one must be extremely cautious in estimating the kinematic characteristics of rail-gun accelerators of solid bodies with a plasma piston in the motion of the mass center approximation (as is now widely done in the literature).

LITERATURE CITED

1. S. C. Rashleigh and R. A. Marshall, "Electromagnetic acceleration of microparticles to high velocities," *J. Appl. Phys.*, **49**, 2540 (1978).
2. V. M. Titov and G. A. Shvetsov, "Acceleration of macroparticles to high speeds," in: *Dynamics of Continuous Media* [in Russian], Inst. Gidrodin. Sib. Otd., Akad. Nauk SSSR, No. 78, Novosibirsk (1986).
3. R. S. Hawke, W. J. Nellis, et al., "Rail accelerator development for ultrahigh-pressure research," *IEEE Trans. on Magnetics*, **MAG-20**, No. 2 (1984).
4. W. E. Fox, C. E. Cummings, et al., "Mechanical design aspects of the HYVAX railgun," *IEEE Trans. on Magnetics*, **MAG-20**, No. 2 (1984).
5. S. Usuba, K. Kondo, and A. Sawaoka, "Status of electromagnetic mass-accelerator development and prospect of application to high-pressure research," in: *Shock Waves in Condensed Matter: Proc. APS Top. Conf.*, Santa Fe (1983).
6. R. S. Hawke, A. C. Brooks, A. Mitchel, et al., "Railguns for equation-of-state research," *Tech. Rep. UCRL-85298* (1981).
7. R. S. Hawke and J. K. Scudder, "Magnetic propulsion railguns: their design and capabilities," in: *Megagauss Physics and Technology, Proc. Conf.*, Washington, 1979, Plenum Press, New York-London (1980).

8. C. M. Fowler, D. R. Peterson, R. S. Hawke, et al., "Railgun development for EOS research," in: Shock Waves in Condensed Matter, AIP Conf. Proc., N. Y. (1982).
9. R. L. Langlin, J. H. Gully, K. E. Nalty, and R. C. Zowarka, "System of the ultrahigh-velocity GEDI experiment," IEEE Trans. on Magnetics, MAG-22, No. 6 (1986).
10. G. A. Shvetsov, V. M. Titov, A. G. Anisimov, et al., "Railgun accelerators of macro-particles. Part I, General characteristics," in: Megagauss Technology and Pulsed Power Applications: Proc. Conf. Santa Fe, 1986, Plenum Press, New York-London (1987).
11. G. A. Shvetsov, V. M. Titov, A. G. Anisimov, et al., "Railgun accelerators of macroparticles. Part II, Experimental investigations," in: Megagauss Technology and Pulsed Power Applications: Proc. Conf. Santa Fe, 1986, Plenum Press, New York-London (1987).
12. G. A. Lyubimov and V. M. Rakhovskii, "The cathode spot of a vacuum arc," Usp. Fiz. Nauk, 125, No. 4 (1978).
13. G. A. Shvetsov, V. M. Titov, et al., "Investigation of the operation of a rail-gun accelerator of solid bodies with a feed from an explosive MHD generator," in: Superhigh Magnetic Field. Physics, Technology, Applications [in Russian], Nauka, Moscow (1984).

PENETRATION OF A STRONG BARRIER BY A SHAPED CHARGE JET

S. A. Kinelovskii and K. K. Maevskii

UDC 539.374

The hydrodynamic theory of detonation quite reliably describes the penetration of a shaped charge jet (SCJ) at sufficiently high penetration velocities. However, a marked difference between the theory and experiment [1-5] is seen with a reduction in velocity. This can be attributed to the actual effect of cohesive forces. An accurate empirical check of the hydrodynamic theory of penetration was made in [3] and a modification of this theory was proposed to consider the effect of the strength of the materials of the jet and the barrier (similar results were obtained independently by N. A. Zlatin). This modification consists of introducing "resistance" into the equation describing flow - the Bernoulli equation. It was noted in [4] that in the penetration of an object by an SCJ, the strength of the jet material need not be considered (a similar proposition was used in [5]). As a result, a formula is obtained which expresses the connection between the velocity V_j of the jet, the penetration velocity V_b , and the strength characteristic of the barrier material:

$$V_b = \frac{\lambda V_j}{\lambda^2 - 1} \left[\lambda - \sqrt{1 + (\lambda^2 - 1) \frac{2H_D}{\rho_j V_j^2}} \right], \quad V_b = \frac{1}{2} V_j \left(1 - \frac{2H_D}{\rho_j V_j^2} \right). \quad (1)$$

Here, H_D is the effective value of the dynamic hardness of the barrier material; $\lambda = \sqrt{\rho_j / \rho_b}$; ρ_j and ρ_b are the densities of the jet and the barrier. The second expression in (1) pertains to the case $\lambda = 1$. Equation (1) (below - model 1) represents one of the most widely used approaches to allowing for cohesive forces on the process of SCJ penetration.

In [4], yet another modification of the hydrodynamic theory was proposed. This modification leads to the formula (model 2)

$$V_b = \frac{\lambda}{1 + \lambda} V_j \sqrt{1 - 2H_D / (\rho_j V_j^2)}. \quad (2)$$

Comparison of (1) and (2) shows that the SCJ ceases to penetrate the barrier at the same critical jet velocity ($V_{j*} = \sqrt{2H_D / \rho_j}$) in both models, although the character of the effect of strength on the penetration process is described differently by each model. Penetration velocity begins to decrease at markedly lower jet velocities in model 1 than in model 2, i.e., the latter is characterized by a stronger "strength-engaging mechanism."

Novosibirsk. Translated from Zhurnal Prikladnoi Mekhaniki i Tekhnicheskoi Fiziki, No. 2, pp. 150-156, March-April, 1989. Original article submitted March 21, 1988; revision submitted May 11, 1988.